IAI
Journals.ASM.org

The *Helicobacter pylori* Autotransporter ImaA (HP0289) Modulates the Immune Response and Contributes to Host Colonization

William E. Sause, Andrea R. Castillo,* and Karen M. Ottemann

Department of Microbiology and Environmental Toxicology, University of California, Santa Cruz, Santa Cruz, California, USA

The human pathogen *Helicobacter pylori* employs a diverse collection of outer membrane proteins to colonize, persist, and drive disease within the acidic gastric environment. In this study, we sought to elucidate the function of the host-induced gene *HP0289*, which encodes an uncharacterized outer membrane protein. We first generated an isogenic *H. pylori* mutant that lacks *HP0289* and found that the mutant has a colonization defect in single-strain infections and is greatly outcompeted in mouse coinfection experiments with wild-type *H. pylori*. Furthermore, we used protease assays and biochemical fractionation coupled with an HP0289-targeted peptide antibody to verify that the HP0289 protein resides in the outer membrane. Our previous findings showed that the *HP0289* promoter is upregulated in the mouse stomach, and here we demonstrate that *HP0289* expression is induced under acidic conditions in an ArsRS-dependent manner. Finally, we have shown that the *HP0289* mutant induces greater expression of the chemokine interleukin-8 (IL-8) and the cytokine tumor necrosis factor alpha (TNF-α) in gastric carcinoma cells (AGS). Similarly, transcription of the IL-8 homolog keratinocyte-derived chemokine (KC) is elevated in murine infections with the HP0289 mutant than in murine infections with wild-type *H. pylori*. On the basis of this phenotype, we renamed HP0289 ImaA for immunomodulatory autotransporter protein. Our work has revealed that genes induced *in vivo* play an important role in *H. pylori* pathogenesis. Specifically, the outer membrane protein ImaA modulates a component of the host inflammatory response, and thus may allow *H. pylori* to fine tune the host immune response based on ImaA expression.

The human pathogen *Helicobacter pylori* infects half of the world's population and causes chronic infection that elevates the risk of multiple gastric diseases, including gastric adenocarcinoma (30, 54, 73). In an effort to better understand *H. pylori* pathogenesis, Castillo et al. identified a set of *H. pylori* genes that were expressed at higher levels when the bacterium was in the mouse stomach than when the bacterium was in the lab setting. Host-induced genes have been shown to be crucial for colonization and virulence in a number of bacterial species, including *H. pylori* (15–17, 35, 44, 49, 66, 78). This previous work used recombination-based *in vivo* expression technology (RIVET) to identify host-induced *H. pylori* genes (17). The RIVET system utilizes fusions of transcriptional promoters to a promoterless gene encoding a recombinase protein. If these promoters are transcribed, for example in the mouse stomach, the recombinase is created and mediates site-specific recombination events that convert the strain from antibiotic resistance to antibiotic sensitivity (71). The previous study analyzed ~71% of the genome and found six promoters induced *in vivo* (17). Two of the promoters (P*ivi10* and P*ivi66*) regulated genes, *mobABD* and *cagZ*, respectively, that were important for mouse stomach colonization (17). Of the four remaining unstudied promoters from the RIVET screen, one regulated a gene, *HP0289*, that was previously annotated as a toxin-like outer membrane protein in the complete genome sequence of *H. pylori* strain 26695 (67). Here we explore how *HP0289* contributes to *H. pylori* pathogenesis.

The *H. pylori* genome is predicted to encode more than 30 outer membrane proteins (OMPs), or approximately 4% of the bacterium's coding potential (3, 23). This level of dedication to *omp* genes is not commonly seen in other bacterial species, and only a small percentage of these OMPs have actually been characterized in *H. pylori* (3, 7, 23, 29). The abundance of specialized OMPs in the *H. pylori* proteome has been proposed to allow the bacterium to persist within an environment that is demanding and often changing (39). Of the well-studied *H. pylori omp* genes, a number encode proteins that play a prominent role in *H. pylori* pathogenesis (29). The most notable of these proteins include the vacuolating cytotoxin protein VacA and the host antigen-specific adhesins BabA and SabA. VacA belongs to a family of OMPs called autotransporters, a class of proteins that appear three other times in the *H. pylori* proteome (26). While a number of *H. pylori* OMPs have been characterized, VacA is the only OMP with an autotransporter domain that has been well described; thus, a void exists in our knowledge of the remaining autotransporters.

Autotransporters are a family of Gram-negative bacterial secreted proteins that can be toxins, proteases, or adhesins (23, 28). These proteins are called autotransporters because originally they were thought to contain all of the machinery necessary for secretion to the outer membrane. Recent work, however, suggests that many interact with an additional protein, the beta-barrel assembly machinery BAM (29, 65). All autotransporters possess a conserved domain structure, which consists of the following: (i) an N-terminal signal peptide that facilitates Sec-dependent secretion across the inner membrane; (ii) a generally nonconserved central region called the passenger domain, which confers the effector function of the protein; and (iii) a C-terminal beta-barrel domain

Received 27 March 2012 **Returned for modification** 18 April 2012
Accepted 27 April 2012
Published ahead of print 7 May 2012
Editor: S. R. Blanke
Address correspondence to Karen M. Ottemann, ottemann@ucsc.edu.
* Present address: Biology Department, Eastern Washington University, Cheney, Washington, USA.

doi:10.1128/IAI.00312-12

TABLE 1 *H. pylori* strains used in this study

Strain	Description or relevant genotype	Reference
G27	Wild type (NSH57 parent strain)	19
NSH57	Mouse-adapted isolate of G27	8
LSH100	NSH57 with repaired *fliM* allele	50
SS1	Wild type	42
26695	Wild type	1
KO954	SS1 Δ*imaA*::*cat*	This study
KO1370	LSH100 Δ*imaA*::*cat*	This study
KO1371	LSH100 Δ*arsS*::*cat*	This study
KO1163	SS1 *cagE*::*kan*	This study (strain provided by David McGee)
KO1372	LSH100 *cagE*::*kan*	This study
KO1373	LSH100 *cagE*::*kan* Δ*imaA*::*cat*	This study
KO1374	26695 Δ*imaA*::*cat*	This study

that is the hallmark of the autotransporter family and is critical for protein translocation across the outer membrane (29). Passenger domains represent the surface-exposed component of the protein and typically adopt an extended right-handed beta helix structure (11, 82). These domains are extremely diverse in both sequence and function, making it difficult to predict what a particular autotransporter does (29). Known autotransporter functions include the following: (i) binding to host proteins to mediate adhesion, invasion, immunoglobulin binding, or intracellular movement; (ii) interacting with other bacterial molecules to mediate agglutination and biofilm formation; (iii) acting as intracellular toxins; and (iv) behaving as proteases that target such proteins as host immunoglobulin. The autotransporter studied here, HP0289, was originally annotated as a toxin-like outer membrane protein; however, there is no experimental evidence for such a function (76).

H. pylori colonization causes chronic inflammation, a host response that is considered one of the primary risk factors for adenocarcinoma (30). *H. pylori* strains are highly variable and are well documented to contain various combinations of genes that enhance inflammation, including genes of the *cag* pathogenicity island (*cag*PAI), *oipA*, *babA*, and *sabA* (25, 33, 51, 86). Recent reports suggest that *HP0289* might also vary between strains. Specifically, Kawai et al. analyzed 20 *H. pylori* genome sequences and found that the highly carcinogenic East Asian (hspEAsia lineage) strains had several changes, including a large deletion in *HP0289* that removed 83% of the protein (38). Indeed, Lee et al. previously demonstrated that East Asian clinical isolates induce epithelial cells to produce significantly higher proinflammatory cytokine levels than do Western strains; however, the strains in this specific study were not analyzed for the presence of *HP0289* (43). These findings thus suggest that loss of *HP0289* may create *H. pylori* strains that are more proinflammatory.

In this study, we characterize the *H. pylori* autotransporter HP0289 and show that it contributes to murine stomach colonization and is under the control of the acid-sensing ArsRS two-component system. Additionally, we demonstrate that the protein decreases expression of inflammatory chemokines and cytokines in both cultured epithelial cells and infected stomachs.

MATERIALS AND METHODS

Bacterial strains and growth conditions. All bacterial strains are described in Table 1. *H. pylori* strain LSH100, a mouse-adapted descendant of the clinical isolate G27 (19, 50), was used for proteinase K digestions, all of the mouse colonization, gene expression, and AGS cell experiments. Strain 26695 was used for additional AGS cell inflammation experiments (1), and *H. pylori* strain SS1 (42) was used for murine infection and ImaA subcellular localization experiments. *H. pylori* strains were maintained on Columbia blood agar base (Difco, Detroit, MI) supplemented with 5% defibrinated horse blood (Hemostat Laboratories, Dixon, CA), 0.2% (wt/vol) β-cyclodextrin (Sigma) plus 5 μg/ml trimethoprim, 8 μg/ml amphotericin B, 50 μg/ml cycloheximide, 10 μg/ml vancomycin, 5 μg/ml cefsulodin, and 2.5 U/ml polymyxin B (CHBA) to inhibit the growth of unwanted microbes under 10% CO_2, 7 to 10% O_2 and balance N_2, at 37°C. Liquid *H. pylori* cultures were grown in 1× Ham's F-12 medium (Gibco, Grand Island, NY) containing 10% heat-inactivated fetal bovine serum (FBS) (Gibco) or brucella broth supplemented with 10% fetal bovine serum (BB10). The antibiotic chloramphenicol (Cm) was used for selection at a concentration of 13 μg/ml. *H. pylori* strains were stored at −80°C in brain heart infusion medium supplemented with 10% fetal bovine serum, 1% (wt/vol) β-cyclodextrin, 25% glycerol, and 5% dimethyl sulfoxide.

Acid exposure. *H. pylori* bacteria cultured for ~36 h on CHBA were resuspended in sterile BB10, and their concentrations were determined by optical density (optical density at 600 nm [OD_{600}]). For the 2-h acid treatment to examine *imaA* and *ureA* transcript levels, the cell suspensions were diluted to an OD_{600} of 1.75 in 1 ml of BB10 and then centrifuged at 2,500 × *g* for 8 min. The resulting pellet was resuspended in 2 ml of BB10 at a pH of either 5 or 7 and then incubated at 37°C under *H. pylori* culture conditions for 2 h. For the time course experiments measuring ImaA protein levels, cells were prepared the same way, except that the cultures were diluted to an OD_{600} of 0.220 at the initiation of the incubation period. The cell density of each sample taken at every time point was then normalized with the OD_{600} to ensure that equal amounts of protein were being examined for each respective culture.

Mammalian cell culture. AGS (ATCC CRL 1739) human gastric epithelial cells were obtained directly from the American Type Culture Collection (ATCC) and maintained in Dulbecco's modified Eagle's medium (DMEM) (Lonza, Walkersville, MD) containing 10% FBS at 37°C with 10% CO_2. To assay interleukin-8 (IL-8) production, AGS cells were seeded at 1×10^5 cells/ml in 24-well tissue culture dishes and incubated for 24 h. After this period, *H. pylori*, cultured for ~36 h on CHBA, were scraped from a plate and resuspended in sterile DMEM plus FBS to a concentration of 1×10^7 to create a multiplicity of infection (MOI) of 100. *H. pylori* concentrations were determined by OD_{600}, assuming 3×10^8 bacteria/ml/OD_{600} unit. AGS cells were infected for 2 h under 10% CO_2. After 2-h incubation, culture supernatant was removed, and AGS monolayers were washed twice in 1× phosphate-buffered saline (PBS), and then the cells were resuspended in TRIzol for RNA isolation.

Construction of *H. pylori* mutants. *H. pylori* SS1 Δ*imaA*::*cat* mutant was created using splicing by overlap extension (SOE) PCR with the primers D1 (5′-GCCCTTAGTTCAGGTGTGGCAGTTTAAGG), D2 (5′-CAAGGAGGATCCCGGCCGCGGCTACCTTCTCATTTCCTAGATAGTAGCC), D3 (5′-ATCCACTTTTCAATCTATATCACGGTTGCCGGGAATGTGGGCATGCGAGTGGCG), and D4 (5′-GTTTTAGCGTCAATGTTGGGGTTGATTCTAATGG) that amplified the *imaA* chromosomal region and primers catF (F stands for forward) (17) and catR2 (R stands for reverse) (17) that amplified the *cat* gene. This gene deletion extends from 7 bp upstream of the *imaA* start codon to 31 bp upstream of the *imaA* stop codon and places a terminatorless *cat* gene in the same transcriptional orientation as *imaA*. To generate the deletion in *H. pylori* LSH100, genomic DNA from *H. pylori* SS1 Δ*imaA*::*cat* mutant was used to naturally transform wild-type strain LSH100 to create strain KO1370 (KO stands for knockout). The deletion in 26695 was produced by natural transformation of wild-type 26695 with genomic DNA from strain KO1370, to generate strain KO1374. Selection was done on CHBA containing Cm, and proper integration was confirmed with PCR using primers D4 and catR2. To generate the LSH100 Δ*arsS*::*cat* mutant (KO1371),

the chloramphenicol resistance cassette (*cat*) was inserted into the *arsS* gene (HP0165) by SOE PCR. In brief, primers were generated that reside approximately 300 bp upstream of *arsS*, ArsS1.1 (5′-AACCCTATGATC CTAAGGAATTA) and ArsS3.1 (5′-ATCCACTTTTCAATCTATATCAA CGCAAAACCCCTTAACTCC), and downstream of *arsS*, ArsS2.2 (5′-G GCTTCCTGTAGCGTCCTTATG) and ArsS4.1 (5′-CCCAGTTTGTCG CACTGATAAGAGAACATGTTCAAACGATTGA). The two *arsS* PCR products were spliced to a third PCR product that contained the nonpolar *cat* allele generated from the primers catR2 and catF (17). The PCR product composed of the *cat* gene flanked by upstream and downstream regions of the *arsS* gene was then cloned into the TOPO-TA vector (Invitrogen) to generate plasmid p*cat-arsS*. This plasmid was then used to naturally transform strain LSH100 to Cm resistance. Proper integration was confirmed by PCR using primers ArsS1.1 and ArsS2.2 and by sequencing of that PCR product. The original *cagE* mutant was a kind gift from David McGee and Kylie Nolan (Table 1). It consists of an insertion of the *aphA3* gene at a unique BglII site in *cagE* (HP0544, cag23) that is ~600 bp from the start site of the 3,000-bp gene. We used genomic DNA from this strain to naturally transform either wild-type strain LSH100 or mutant strain KO1370 to kanamycin resistance.

Mouse colonization experiments. *H. pylori* strains used for colonization analyses were passaged minimally in the lab (two or three times) and then inoculated into either Ham's F-12 culture medium (75) for *H. pylori* LSH100 or BB10 for *H. pylori* SS1 for ~18 h, as described above. After this period, cells were analyzed to determine motility and cell concentration (OD_{600}) prior to infection. For all infections, 4- to 6-week-old male FVB/N mice (Charles River) were housed in an Association for the Assessment and Accreditation of Laboratory Animal Care-accredited facility in microisolator cages with free access to standard food and water. All animal procedures were approved by the Institutional Animal Care and Use Committee. Approximately 1 ml of *H. pylori* cells containing 9×10^7 to 1×10^8 CFU/ml were used to orally gavage the mice. For coinfections, wild-type and mutant cells were grown separately and then combined in equal concentrations. To determine the true CFU/ml of each culture, all cultures were serially diluted and plated on CHBA. Infections were allowed to persist for 2 to 3 weeks, after which time mouse stomachs were excised as described before (57), homogenized using the Bullet Blender (Next Advance, Averill Park, NY), and then plated on CHBA with or without Cm (described above) supplemented with 10 μg of nalidixic acid/ml and 200 μg of bacitracin/ml. For the coinfection, the mouse stomachs were plated on both nonselective CHBA and CHBA supplemented with Cm as described previously (74). The cell counts obtained from the input and output data allowed us to calculate the competitive index, as follows: (CFU/g of mutant strain output/CFU/g of wild-type strain output)/(CFU/g of mutant strain input/CFU/g of wild-type strain input).

For keratinocyte-derived chemokine (KC) (mouse IL-8 homolog) detection in mouse tissue, infections persisted for 3 weeks (2). When excising the stomach, half of the tissue was placed in BB10 for plating and the other half was placed immediately in liquid N_2 and then stored at −80°C within an hour of extraction. To isolate RNA, tissue samples were suspended in TRIzol and then homogenized using the Polytron (Kinematica, Switzerland) automated tissue homogenizer.

RNA preparation. Total RNA was isolated from *H. pylori* strains LSH100 and its isogenic mutants, Δ*imaA*::*cat* and Δ*arsS*::*cat* mutant strains, using TRIzol reagent (Invitrogen, Carlsbad, CA) combined with RNeasy columns (Qiagen, Valencia, CA). Bacterial cells were pelleted and resuspended in 1 ml of TRIzol at room temperature for 5 min before 200 μl of chloroform was added. Samples were then centrifuged (12,000 × *g*, 15 min, 4°C), and the aqueous layer was removed and placed into new tubes. RNA was precipitated by combining 500 μl of isopropanol with the aqueous layer and incubating at room temperature for 10 min, followed by a centrifugation as described above. The RNA pellet was washed with 75% ethanol, dried, and resuspended in RNase-free water. To remove contaminating genomic DNA from purified RNA, samples were treated with 4 U of RNase-free DNase I (Ambion) for 3 h at 37°C, followed by further purification using the Qiagen RNeasy spin columns as specified in the manufacturer's instructions. RNA was ultimately eluted in RNase-free water, RNA concentrations were quantified on a Nanodrop spectrophotometer (Nanodrop, Wilmington, DE), and the absence of contaminating genomic DNA was confirmed BY PCR. RNA was immediately transcribed into cDNA (see below), and the remaining sample was stored at −80°C.

RNA was isolated from AGS cells in a similar manner. Briefly, 1 ml TRIzol reagent was added directly to cells in the culture dish per 10 cm^2 of culture dish surface. The cells, including infecting *H. pylori* cells, were lysed directly in the culture dish by pipetting the cells up and down several times. Homogenized samples then underwent the same preparation as described above, except the DNase I treatment and secondary purification with the Qiagen RNeasy kit were omitted.

cDNA synthesis and quantitative real-time PCR. Total RNA served as a template for cDNA synthesis using the Tetro cDNA synthesis kit (Bioline, London, United Kingdom). cDNA synthesis was carried out following the manufacturer's protocol, starting with 0.5 to 1 μg total RNA, 50 ng random hexamers, and 10 mM deoxynucleoside triphosphates (dNTPs) per 20-μl reaction mixture. The mixture was incubated at 65°C for 10 min before being combined with 10 μl of master mix, which includes the reverse transcriptase enzyme (200 U/μl). The reaction proceeded for 1 h at 37°C until the reverse transcriptase enzyme was inactivated at 70°C for 15 min. Quantitative real-time PCR was performed using the Opticon 2 real-time cycler (Bio-Rad, Hercules, CA) and SYBR green supermix reagents (Bioline, London, United Kingdom). For relative expression of *imaA* and *ureA*, transcript levels were normalized to the levels of *groEL* (69) in each sample. Transcripts were amplified with HP0289 For1.1 (For stands for forward) (5′-TAACGATCCAAAACGCT TCC) and HP0289 Rev1.1 (Rev stands for reverse) (5′-TCCCTTGAGGC GAGAGTGATT), UreA F1 and UreA R1 (36), and groEL F (JVO-529) and groEL R (JVO-5298) (69). *Il8* (55) and *TNF-α* (84) expression levels from AGS cells were normalized to *18S* (55) rRNA, and KC levels from mouse tissues were normalized to *GAPDH* (24). All reactions were performed in triplicate, and a melting curve analysis was used to ensure that a single product was amplified with each primer set. To validate RNA purity, no reverse transcriptase control reactions were also performed. *imaA* gene expression at low pH was determined from 4 independent experiments, and statistical differences were evaluated with the Mann-Whitney U-test. Relative expression of *Il8* was determined from 5 independent experiments, and statistical differences were evaluated by Student's *t* test. All differences in gene expression were calculated by the $\Delta\Delta C_T$ method (47).

ELISA. Enzyme-linked immunosorbent assays (ELISAs) for human IL-8 were performed using the Human IL-8 EASIA kit (Invitrogen). AGS cells were infected by either wild-type *H. pylori* or its isogenic mutant, Δ*imaA*::*cat* mutant strain, at concentrations of 1×10^7, 2×10^6, and 1×10^5 cells/ml, and culture supernatant was preserved for ELISA at 4, 6, 12, and 24 h postinfection.

Proteinase K treatment of *H. pylori* cells. Digestion of *H. pylori* outer membrane proteins with the extracellular protease, proteinase K, was conducted as described previously by Sabarth et al. (63). *H. pylori* cells grown for 48 h on CHBA plates were collected with an inoculation loop and suspended in 1 ml of phosphate-buffered saline. Cells were centrifuged at 5,000 × *g* for 10 min and then resuspended in PBS at a concentration of 3×10^8 cells/ml, based on the OD_{600}. Cells were treated with either 40 or 400 μg/ml proteinase K for 30 min at room temperature in 1× PBS. The reaction was halted with the addition of 5 mM phenylmethylsulfonyl fluoride (PMSF); the cells were then washed twice in PBS. After a final centrifugation at 5,000 × *g* for 5 min, the cells were resuspended in PBS and then diluted into NuPAGE 4× sample buffer (Invitrogen, Carlsbad, CA) for subsequent Western blot analysis.

Sarcosine preparation of *H. pylori* outer membrane. The sarcosine-insoluble outer membrane fraction was prepared as described previously (7) with slight modifications. *H. pylori* wild-type strain SS1 and its isogenic mutant, Δ*imaA*::*cat* mutant strain, were grown on CHBA for 48 h.

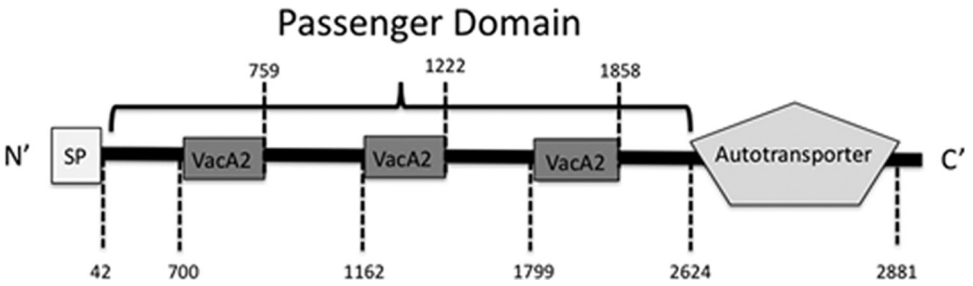

FIG 1 ImaA contains hallmarks of autotransporter proteins. The schematic diagram shows the highly conserved domains in ImaA as predicted by SignalP 3.0 and SMART and the N-terminal (N′) signal peptide (SP) and the C-terminal end (C′). The signal peptide probability was 1.00, and the autotransporter E value was 5×10^{-7}. Numbers below and above the schematic diagram indicate the amino acid positions of predicted domains within ImaA.

To optimize the outer membrane yield, each respective strain was grown to confluent growth on two full CHBA plates, with all of the cells utilized for fractionation. Cells were collected using a sterile inoculation loop and suspended in 1 ml of 20 mM Tris-HCl (pH 7.5) and collected by centrifugation (8,000 × *g*, 10 min, 4°C). The pellet was then resuspended in 1 ml of 20 mM Tris-HCl containing a protease inhibitor (1 mM PMSF) and a cell wall hydrolase (0.25 mg/ml lysozyme). The resuspended pellet was sonicated 9 times for 15 s each time (Fisher sonicator, 80% amplitude), and unbroken bacteria were removed by centrifugation (6,000 × *g*, 10 min, 4°C). Total membranes were isolated by centrifugation for 45 min at 50,000 × *g* and 4°C. The supernatant containing the soluble fraction was removed, and the total membrane pellet was washed once in PBS, resuspended in 1 ml sonication buffer containing 2.0% (wt/vol) sodium lauryl sarcosine, and incubated at room temperature for 30 min. The inner membrane fraction was separated by centrifugation (50,000 × *g*, 45 min, 4°C), and the pellet containing the outer membrane was resuspended in sarcosine for an additional treatment to optimize outer membrane purity. The resuspended pellet was incubated at room temperature for another 30 min and then centrifuged (50,000 × *g*, 45 min, 4°C). The final pellet was resuspended in 1 ml of 20 mM Tris-HCl and stored at −20°C.

Western blotting and ImaA antibody creation. The ani-ImaA-1 polyclonal antibody was prepared in rabbits using a 19-amino-acid peptide (amino acids 2065 to 2084) from the passenger domain of the ImaA protein (Open Biosystems, Huntsville, AL). The antibody specifically recognizes ImaA, as well as several unidentified nonspecific proteins that were significantly different in size.

Proteins for Western blot analysis were resuspended in 4× NuPAGE sample buffer (Invitrogen, Carlsbad, CA) with 0.025% 2-mercaptoethanol and heated at 70°C for 15 min. Samples were separated on 3 to 8% NuPAGE Tris-acetate gels for 60 min at 150 V. Following electrophoresis, the proteins were transferred to polyvinylidene difluoride membranes (Bio-Rad, Hercules, CA) with the Bio-Rad semidry transfer cell for 35 min at 16 V. The membranes were then incubated with a 1:300 dilution of anti-ImaA-1 antibody or a 1:2,000 dilution of anti-GST-TlpA22 (GST stands for glutathione *S*-transferase) antibody (83) for ~18 h at 4°C. For visualization, blots were incubated with goat anti-rabbit antibody conjugated to horseradish peroxidase (Santa Cruz Biotech) at a dilution of 1:2,000 for 1 h, followed by incubation with luminol, *p*-coumaric acid, and hydrogen peroxide. Luminescent blots were visualized by exposure to Ultra Cruz autoradiography film (Santa Cruz Biotech).

RESULTS

***H. pylori* ImaA is predicted to be an autotransporter.** To examine the functional significance of the uncharacterized *H. pylori* genes that were upregulated in the stomach (17), we employed *in silico* sequence analyses of each protein to identify signature domains. The gene predicted to be regulated by promoter P*ivi77*, *HP0289*, is predicted to encode a protein with all of the typical characteristics of an autotransporter (Fig. 1). On the basis of experiments described below, we designate HP0289 as ImaA (immunomodulating autotransporter). *imaA* is transcribed monocistronically (69), and the protein encoded by this gene is 2,893 amino acids in length with a calculated molecular mass of 311 kilodaltons. The SignalP algorithm predicts that ImaA bears an N-terminal signal peptide with a signal peptidase cleavage site between positions 42 and 43 (VYA-NN) (10). ImaA also carries the highly conserved C-terminal beta-barrel autotransporter domain, readily identified by domain finding software such as the Simple Modular Architecture Research Tool (SMART) (67). The passenger domain of ImaA, which likely confers the effector function of the protein, is 2,581 amino acids in length. This region has little conservation with any other previously characterized protein, with the exception of three "VacA2" regions that are 59 amino acids long. In the initial sequencing of *H. pylori*, HP0289 was annotated as a toxin-like protein, with small regions of similarity noted between VacA, HP0289 and two other *H. pylori* autotransporters (HP0610 and HP0922) (76). The main block of homology is at the C-terminal autotransporter domain. There were, however, additional regions of low similarity (26 to 31%) at several spots in the central passenger domain called VacA2 regions, although these regions do not correspond to a functional portion of VacA. Based on this homology, ImaA has been annotated as a VacA paralog. Our analysis, however, suggests that ImaA is an autotransporter that is not specifically related to VacA.

ImaA promotes mouse stomach colonization. RIVET studies in several organisms have identified pathogen colonization and virulence factors (15–17, 44, 49, 66, 78). Therefore, we first examined whether *imaA* was required for mouse stomach colonization, a model routinely utilized in *H. pylori* studies. We generated an *imaA* mutant, Δ*imaA*::*cat*, in which nearly the entire *imaA* open reading frame (ORF) is replaced with the chloramphenicol acetyltransferase (*cat*) gene, and thus is a null allele. This allele was used to replace the endogenous *imaA* locus in the *H. pylori* strain LSH100 (50). LSH100 is a mouse-adapted derivative of *H. pylori* G27 (19). LSH100 arose from mouse adaptation of strain G27 to create strain NSH57, followed by repair of a mutation in the *fliM* locus to the original wild-type sequence to yield LSH100 (50). We used the LSH100 strain, because both it and the original RIVET strain, mG27, were derived from the same parent, but LSH100 infects mice more consistently. Because of their high genetic relatedness, we felt that experiments with both mG27 and LSH100 would not have revealed significantly different conclusions. Unless noted otherwise, all subsequent *in vivo* and *in vitro H. pylori* infections, localization, and gene expression experiments were

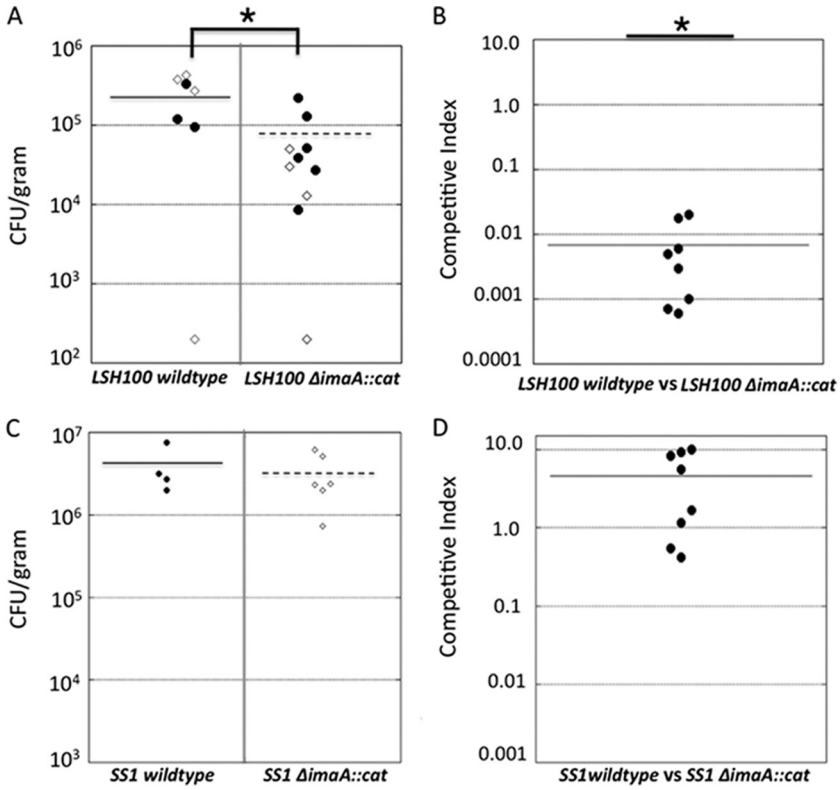

FIG 2 (A) The *H. pylori* LSH100 Δ*imaA*::*cat* mutant colonizes mice at levels significantly lower than those of the wild-type *H. pylori* LSH100 parent. Oral single-strain infection studies with the wild-type *H. pylori* or Δ*imaA*::*cat* mutant were carried out using male FVB/N mice. Infections persisted for 2 or 3 weeks. Single-strain infections were conducted with 7 mice for the wild-type strain and with 10 mice for the Δ*imaA*::*cat* mutant. Each circle represents the value for one infected mouse, derived from independent 2-week (open circles) or 3-week (filled circles) infections, and the solid or broken line represents the mean for the group of mice. The values between the two groups of mice in panel A were significantly different ($P = 0.01$ by Student's *t* test) and are indicated by the bracket and asterisk. (B) The *H. pylori* LSH100 Δ*imaA*::*cat* mutant is outcompeted by the wild-type strain in a coinfection colonization assay. Each point represents the competitive index for one mouse stomach for eight mice in two independent infections. The competitive index is a ratio and is calculated as follows: (mutant output/wild-type output)/(mutant input/wild-type input). The values were significantly different ($P < 0.001$ by Student's *t* test) compared to a hypothetical strain with no defect (competitive index [CI] of 1). (C) The *H. pylori* SS1 Δ*imaA*::*cat* mutant colonizes mice at levels that are comparable to those of wild-type *H. pylori* SS1. These infections persisted for 2 weeks, with four mice for the wild-type strain and six mice for the Δ*imaA*::*cat* mutant strain. (D) The *H. pylori* SS1 Δ*imaA*::*cat* mutant is not outcompeted for mouse colonization in a coinfection with wild-type *H. pylori* in two independent infections of eight mice.

done with strain LSH100 to maintain consistency with our mouse-infecting strain. Male FVB/N mice were infected with wild-type LSH100 or its isogenic Δ*imaA*::*cat* mutant for 2 to 3 weeks. These time points have been widely used in other *H. pylori* murine colonization studies and have been shown to accurately reflect colonization levels at longer infection time points (8, 18, 27, 52, 58, 72, 74, 80). While the *imaA* mutant was able to sustain infection for these lengths of time, the output CFU/gram stomach was significantly lower than that obtained from wild-type infections (Fig. 2A). To address whether the colonization defect of the Δ*imaA*::*cat* strain would be altered by the presence of wild-type *H. pylori*, we carried out coinfection experiments with equal concentrations of wild-type and Δ*imaA*::*cat* strains. Two weeks postinfection, we determined the ratio of CFU/g of stomach for mutant and wild-type bacteria and calculated a competitive index. In all infections, the *imaA* mutant was greatly outcompeted by the wild-type bacteria (Fig. 2B). These results demonstrate that *H. pylori* requires ImaA to reach wild-type gastric colonization levels. We did not complement the *imaA*::*cat* mutant, because *imaA* is over 8,000 base pairs in length and therefore would be readily targeted by *H. pylori*'s extensively developed restriction-modification system, which comprises over 4% of the genome (46). Despite advances in methods to circumvent the *H. pylori* restriction-modification system, gene complementation remains one of the most difficult endeavors in *H. pylori* molecular genetics (22).

ImaA has been shown to be important in other *H. pylori* strains. Specifically, an *imaA* (HP0289) transposon mutant in *H. pylori* strain G1.1 was outcompeted by the wild-type *H. pylori* strain for gerbil colonization (37). To expand this analysis, we checked whether a third strain, SS1, would similarly need *imaA* for stomach colonization. We found, surprisingly, that *H. pylori* SS1 Δ*imaA*::*cat* colonized as well as the wild type did in both single-strain and competition infections (Fig. 2C and D). This strain difference is not surprising, given that others have observed that there is extensive variability in whether particular *H. pylori* proteins are essential for mouse colonization (8). Thus, these results suggest that ImaA is needed by some strains and that ImaA's importance is possibly dependent on each strain's unique interactions with the host.

ImaA is secreted to the outer membrane of the cell. We next wanted to confirm the *in silico* prediction that ImaA is exported to the outer membrane of the cell. We first generated a peptide anti-

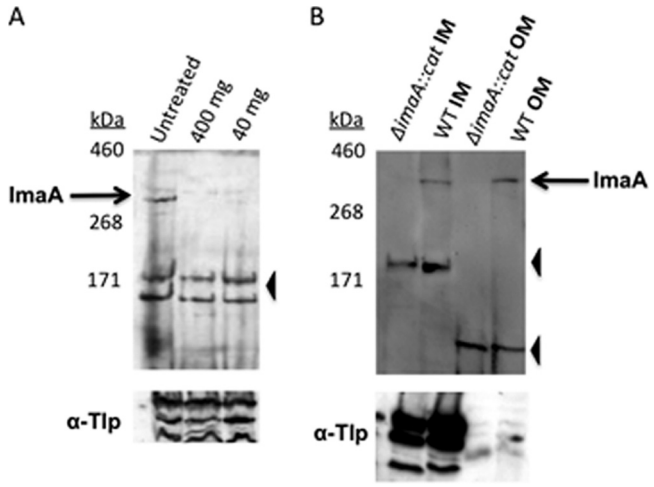

FIG 3 ImaA localizes to the outer membrane. (A) Whole cells of *H. pylori* strain LSH100 were treated with different concentrations of proteinase K (40 or 400 mg ml^{-1}) or with no proteinase K as a control. The top panels show blots probed with anti-ImaA-1, while the bottom panels are probed with anti-GST-TlpA22 antibody (α-Tlp), which recognizes inner membrane chemoreceptors (83). Similar results were obtained with strain mG27 (not shown). (B) Sarcosine-insoluble outer membrane (OM) fractions and sarcosine-soluble inner membrane (IM) fractions were obtained from wild-type (WT) and *H. pylori* SS1 Δ*imaA*::*cat* mutant cells and then probed with anti-ImaA-1. In both panels, the positions of full-length ImaA are indicated by black arrows labeled ImaA, and the positions of nonspecific proteins recognized by the anti-ImaA serum are indicated by black arrowheads.

body directed at the passenger domain of the protein that accurately detects mature ImaA protein from whole-cell lysates (Fig. 3). We then used proteinase K digestion to assess whether ImaA was surface localized in *H. pylori* LSH100 and mG27. Proteinase K does not diffuse across the outer membrane of Gram-negative bacteria and thus cleaves only proteins residing on the bacterial surface. This approach has been widely used to assess autotransporter surface localization (20, 45, 77). As predicted for a surface-localized protein, ImaA is digested by the protease and is thus surface exposed in strain LSH100 (Fig. 3A) as well as in strain mG27 (not shown). To demonstrate that proteinase K treatments were not breaching the membrane and degrading internal proteins, we determined that the TlpABC chemoreceptors localized on the inner membrane were not digested (Fig. 3A). To further validate these findings and to assess whether ImaA localization to the outer membrane is conserved in strain SS1, we performed subcellular fractionation experiments with the detergent sarcosine, which selectively solubilizes the inner membrane and thus enables separation from the outer membrane. Western blot analysis demonstrated that ImaA is in the outer membrane fraction, as well as somewhat in the inner membrane (Fig. 3B). A control blot, using antibody that detects the inner membrane protein, showed that the fractions were fairly pure (Fig. 3B). Inner membrane-localized ImaA may represent protein that is transiting to the outer membrane or an indication of incomplete membrane separation. Other studies have detected autotransporter proteins in both inner and outer membrane fractions (5). Of note, these analyses were performed in three different *H. pylori* strain backgrounds, providing strong evidence that ImaA is translocated to the outer membrane. In addition, we did not detect any ImaA in concentrated supernatant from *H. pylori* cultures (data not shown), suggesting that ImaA stays associated with the outer membrane.

ImaA is a member of the acid-responsive ArsRS regulon. The RIVET studies showed that *imaA* transcription is upregulated within the host environment (17). Therefore, we wanted to identify the signal responsible for inducing *imaA in vivo*. In a recently published *H. pylori* whole transcriptome paper, Sharma et al. demonstrated that *imaA/hp0289* is induced 10-fold at low pH (69). Acidic pH is the key environmental signal for activating the *H. pylori* two-component regulatory system ArsRS (acid-responsive signaling) (60, 62). We thus examined whether *imaA* is a member of the ArsRS regulon by creating a null mutant for the histidine kinase ArsS and observing *imaA* gene expression through quantitative real-time PCR (qRT-PCR) under neutral and acidic conditions. The response regulator, ArsR, is an essential gene so the ArsS mutant serves as the ArsRS representative (9). We employed the housekeeping gene, *groEL*, for normalization, as used in previous work (69). After 2 h of acidic pH exposure, *imaA* expression increased ~10-fold in the wild-type background but not in the *arsS* mutant (Fig. 4A). Furthermore, *imaA* expression is depressed in the *arsS* deletion strain, even at neutral pH (Fig. 4A). These results suggest that *imaA* is a member of the ArsRS regulon. We additionally compared the expression of *imaA* to that of a known ArsRS-regulated acid-induced gene, *ureA* (61). We found that *ureA* gene expression in wild-type *H. pylori* was induced ~14-fold in acid over expression at neutral pH in a partially *arsS*-dependent manner (Fig. 4B), similar to the findings of Pflock et al. (59). At neutral pH, *ureA* required ArsS for expression more so than *imaA* did. These results thus show that the experimental conditions affect ArsS regulon members as expected. Furthermore, our data support that *imaA* is a member of the ArsRS regulon, due to the ArsS-dependent increased expression in acid, but that it is not regulated identically to *ureA*.

We next examined whether ImaA protein levels were affected by pH. For these experiments, we grew *H. pylori* cultures at pH 5 and then sampled them after 2, 5, or 8 h. Despite observing a 10-fold increase in *imaA* mRNA (Fig. 4A), we did not detect any elevation in ImaA protein levels at low pH (Fig. 4C). We did observe, however, that ImaA protein expression was *arsS* dependent at low pH (Fig. 4D). This observation suggested that *H. pylori* relies on ArsRS to maintain ImaA expression under acidic conditions. All together, these results thus show that acid induces *imaA* transcription and that ArsRS is needed to maintain both *imaA* transcript and ImaA protein levels at acidic pH.

Loss of *imaA* creates *H. pylori* strains that induce elevated *Il8* transcription. We next examined whether loss of *imaA* influenced levels of inflammatory mediators in mouse and *in vitro* cell culture models. Colonization of *H. pylori* in the stomach results in the release of the chemoattractant IL-8 in humans or its analog, KC, in mice. IL-8 stimulates the infiltration of neutrophils into the gastric mucosa, leading to chronic inflammation (31, 56); therefore, *Il8* transcription levels are often used as a readout for a pro-inflammatory response (41). To examine ImaA's influence on *Il8*/*KC* levels, we performed *KC* or *Il8* qRT-PCR on mouse tissue or AGS gastric epithelial cells infected with *H. pylori*. In mice infected with *H. pylori* LSH100 (wild-type) or Δ*imaA*::*cat* mutant strains for 3 weeks, a time point used by others for similar analyses (2), we found very low levels of *KC* overall. There was, however, elevated *KC* in mice infected with *H. pylori* Δ*imaA*::*cat* compared

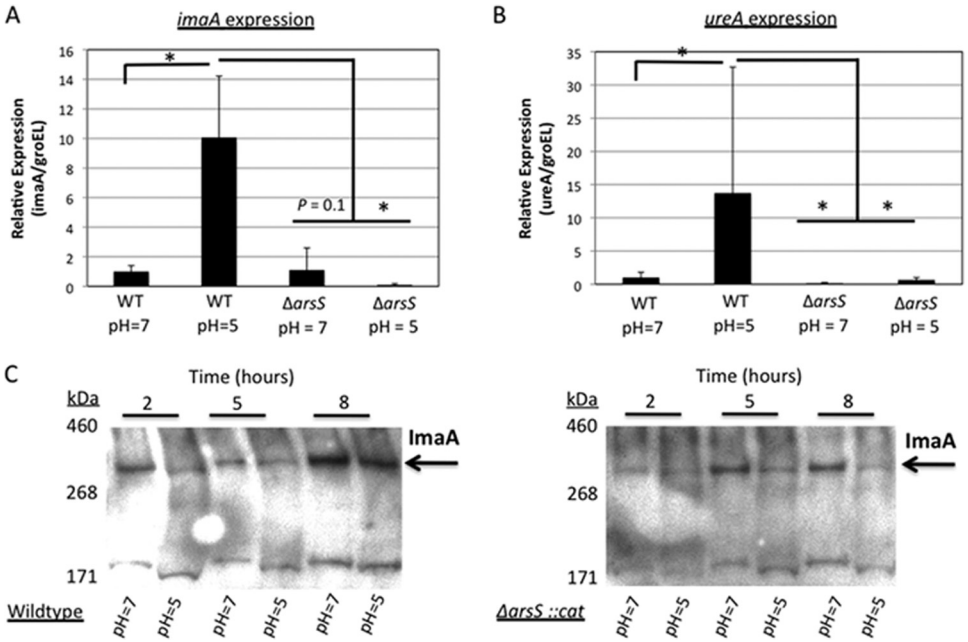

FIG 4 The ArsRS two-component regulatory system influences *imaA* transcription. (A) Quantitative real-time PCR (qRT-PCR) was performed using cDNA generated from the *H. pylori* LSH100 strain or its isogenic mutant, Δ*arsS*::*cat* mutant, that were exposed to either neutral or acidic BB10 for 2 h. The levels of expression of the genes in the wild type (WT) at pH 5 and in the Δ*arsS*::*cat* mutant at pH 5 are shown relative to the values for the WT at pH 7 from four independent biological replicates, each performed in triplicate, and normalized to the housekeeping gene *groEL*. Values for *imaA* expression that are significantly higher or lower ($P < 0.05$ by Wilcoxon rank sum test) are indicated by an L-shaped bracket and asterisk. (B) The *ureA* gene responds to acid and depends on the ArsRS regulatory system for expression. qRT-PCR was performed with the same cDNA that was used in the *imaA* transcription analysis, four independent biological replicates, each performed in triplicate. Values for *ureA* expression that are significantly higher or lower ($P < 0.05$ by Wilcoxon rank sum test) are indicated by an L-shaped bracket and asterisk. (C) Western blots with the anti-ImaA-1 antibody showing ImaA expression at multiple time points under both neutral and acidic conditions in strain LSH100 or in the Δ*arsS*::*cat* mutant strain. These data are representative of the results of three independent time course experiments.

to those infected with the wild-type strain (Fig. 5A). While the difference in *KC* levels between uninfected mice and mice infected with the Δ*imaA*::*cat* mutant was significant, there was minimal difference in KC levels between uninfected mice infected and mice infected with wild-type *H. pylori* (Fig. 5A). These experiments thus suggest that ImaA's normal function is to decrease *KC* levels. To confirm this finding, we employed the well-established AGS human gastric cell model to investigate *Il8* levels. AGS cells infected with wild-type *H. pylori* for 2 h revealed an ~75-fold induction in *Il8* transcription in AGS cells compared to the uninfected cells, while the Δ*imaA*::*cat* mutant strain generated a significantly greater ~189-fold induction in *Il8* levels (Fig. 5B). To confirm that *Il8* transcript levels seen in Δ*imaA*::*cat* mutant infections translated to increased levels of the protein product, we next measured secreted IL-8 levels with an ELISA. *Il8* transcript levels were measured from AGS cells that were infected with *H. pylori* at an multiplicity of infection (MOI) of 100; however, when we measured IL-8 protein levels at this MOI, we saw no difference in cytokine production between Δ*imaA*::*cat* mutant and wild-type *H. pylori* infections (data not shown). We reasoned that the amount of *H. pylori* might be saturating the IL-8 protein production, so we lowered the MOI. When we used an MOI of 1, we witnessed elevated cytokine levels in the Δ*imaA*::*cat* mutant compared to wild-type *H. pylori* infections at 4, 6, and 12 h postinfection, with hour 12 providing a significant difference in IL-8 between the wild-type bacterial and Δ*imaA*::*cat* mutant infections (Fig. 5C). These data suggest that ImaA serves to modulate the amount of IL-8 that is generated during infection.

We next examined whether the inflammation phenotype associated with the loss of *imaA* in *H. pylori* LSH100 was common to other CagA-positive *H. pylori* strains, so we created an Δ*imaA*::*cat* mutant in the widely used CagA-positive strain, 26695, and performed AGS cell infections. Similar to the response we witnessed with *H. pylori* LSH100, the *H. pylori* 26695 Δ*imaA*::*cat* mutant infections induced higher levels of *Il8* transcription overall than the wild-type *H. pylori* infections did (Fig. 5D). Wild-type *H. pylori* 26695 induced an ~106-fold increase in *Il8* transcription compared to uninfected AGS cells, while the 26695 Δ*imaA*::*cat* mutant generated a significantly greater ~274-fold increase in *Il8* transcription.

In addition to IL-8, *H. pylori* infection promotes the production of numerous proinflammatory cytokines. To test whether the Δ*imaA*::*cat* mutant induces elevated concentrations of other immune mediators, we measured transcript levels of the proinflammatory cytokine tumor necrosis factor alpha (TNF-α). TNF-α is associated with an increased severity and distribution of gastritis in infected individuals (70). We found that AGS cells infected with wild-type *H. pylori* produced an ~7-fold increase in *TNF*-α transcript levels compared to uninfected cells, while AGS cells infected with the Δ*imaA*::*cat* mutant displayed a significantly greater 19-fold increase in *TNF*-α levels (Fig. 5E). Taken together, these results suggest that in the absence of ImaA, there is a stronger induction of the mammalian proinflammatory pathway. When mouse tissue was examined for *TNF*-α, there was no difference in the levels between the uninfected mice and mice infected with either the wild-type or Δ*imaA*::*cat* mutant strain (data not

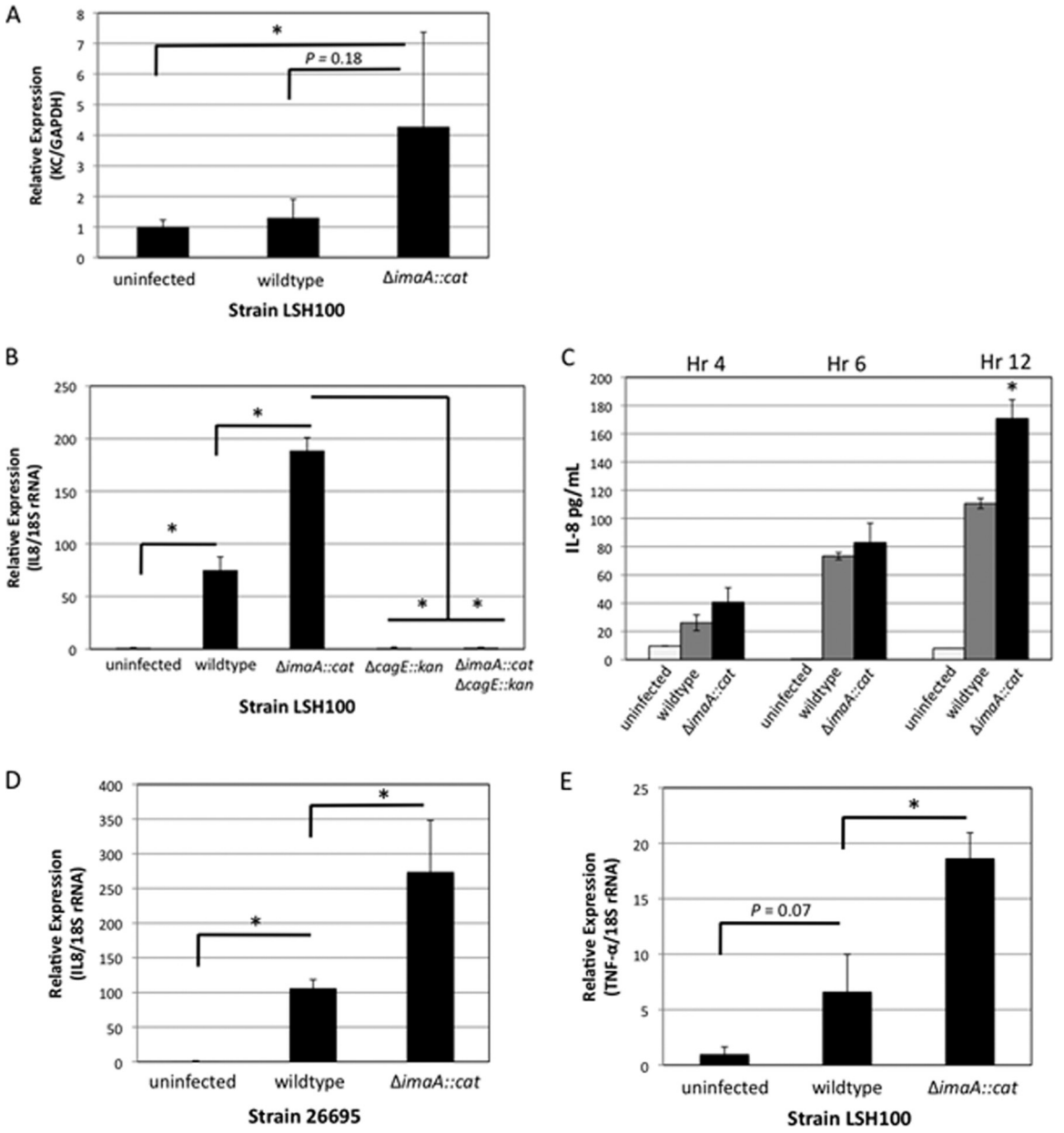

FIG 5 *KC* and *Il8* levels are significantly elevated in Δ*ima*::*cat* mouse and AGS cell infections, respectively. (A) Male FVB/N mice were infected with either the wild-type LSH100 strain or its isogenic mutant, the Δ*imaA*::*cat* mutant, for 3 weeks. Quantitative RT-PCR (qRT-PCR) was performed on whole gastric tissue to analyze the expression of *KC* using primers by the method of Yamaoka et al. (84). Mouse samples are the same as in Fig. 2A and include 5 mice infected with the wild-type LSH100 strain, 8 mice infected with the Δ*imaA*::*cat* mutant, and 6 uninfected mice. There was a significant difference ($P < 0.05$ by Student's *t* test) in *KC* between uninfected mice and mice infected with the Δ*imaA*::*cat* mutant as indicated by the L-shaped bracket and asterisk. (B) *Il8* transcript levels are elevated in AGS cells infected with the Δ*imaA*::*cat* mutant. For transcript analysis, AGS cells were infected with either wild-type LSH100 or its isogenic single mutants, the Δ*imaA*::*cat* or *cagE*::*kan* mutant, or the Δ*imaA*::*cat cagE*::*kan* double mutant at an MOI of 100. qRT-PCR was performed to analyze the expression of interleukin-8 (*Il8*) using primers by the method of Nazarenko et al. (55) after 2 h of infection. These data represent 5 independent infections (biological replicates) with reactions done in triplicate. All differences in expression were calculated by the $\Delta\Delta C_T$ method (47) and statistically significant differences ($P < 0.01$ by Student's *t* test) for AGS cell infections are indicated by an L-shaped bracket and asterisk. (C) ELISAs for IL-8 levels were conducted on culture media taken from AGS cells infected with either wild-type *H. pylori* or with the Δ*imaA*::*cat* mutant (MOI of 1) at the following time points: 4, 6, and 12 h postinfection. Data show two biological replicates, each done with two technical replicates. Values that were statistically significantly different ($P < 0.03$ by Wilcoxon rank sum test) are indicated by an asterisk. (D) *Il8* expression levels in AGS cells infected with either wild-type strain 26695 or its isogenic mutant, the Δ*imaA*::*cat* mutant strain. Data represent 5 independent infections with reactions done in triplicate. The differences in expression were analyzed by the $\Delta\Delta C_T$ method (47). Values that were statistically significantly different ($P = 0.01$ by Student's *t* test) are indicated by an L-shaped bracket and asterisk. (E) Analysis of *TNF*-α transcript levels in AGS cells infected with wild-type LSH100 or its isogenic mutant, the Δ*imaA*::*cat* mutant strain. Data represent 5 independent infections with reactions done in triplicate. The differences in expression were analyzed by the $\Delta\Delta C_T$ method (47). Values that were statistically significantly different ($P < 0.05$ by Student's *t* test) are indicated by an L-shaped bracket and asterisk.

shown). This outcome is not entirely unexpected, as *H. pylori*-induced TNF-α levels appear to be much smaller than *H. pylori*-induced IL-8 levels (85).

The *cag*PAI type IV secretion system underlies the enhanced IL-8 production seen in *imaA* mutant infections. *H. pylori* is known to control IL-8 levels by action of the type IV secretion system (T4SS) encoded by the *cag*PAI. To establish whether the increase in inflammation we witnessed in the Δ*imaA*::*cat* infections was dependent on the activity of the *cag*PAI type IV secretion system (cag-T4SS), we created the Δ*imaA*::*cat* Δ*cagE*::*kan* double mutant and examined *Il8* levels using the same *in vitro* infection model. *cagE* encodes a putative ATPase and is required for IL-8 induction (21). *cagE* mutants had dramatically decreased levels of *Il8* transcription (Fig. 5B), as predicted from other studies with strains related to *H. pylori* G27 (6). The *cagE* effect was dominant over the *imaA Il8* upregulation, as both a Δ*cagE* single mutant and the Δ*cagE* Δ*imaA*::*cat* double mutant induced *Il8* levels that were not significantly above that of the uninfected AGS cells (Fig. 5B). This outcome suggests that the immunomodulatory activity of ImaA requires *cag*PAI function.

DISCUSSION

H. pylori relies on multiple outer membrane proteins to chronically persist within the gastric environment (32, 51, 68). In this study, we demonstrate that a previously uncharacterized *H. pylori* autotransporter, HP0289 or ImaA, is important for host colonization and dampens the inflammatory response. Furthermore, we show that *imaA* is under the control of the acid-responsive ArsRS two-component regulatory system. Our findings thus support the hypothesis that the *in vivo*-induced *imaA* gene contributes to *H. pylori* pathogenesis and that the protein product normally decreases the inflammatory response brought about by the action of the *cag*PAI.

H. pylori must adapt to the changing landscape of the stomach during the course of a chronic infection (12). One way the bacterium can accomplish this adaptation is through tailoring the expression of virulence genes to particular conditions. We found that *imaA* transcription is under the control of the ArsRS regulon. Whole-genome transcriptional profiling of *H. pylori* strains cultured at low pH identified more than 100 genes that were differentially expressed in an *ars*-dependent manner, although *imaA* was not one of them (62). Similarly, others have found that there is some variability in *H. pylori* gene expression at low pH. For example, α-carbonic anhydrase (HP1186) expression has been shown to be repressed in some cases and upregulated in others at low pH (53, 81). We found that *imaA* expression is induced under acidic conditions, similar to the findings of Sharma and colleagues (69), and furthermore, we found that transcriptional control of *imaA* is mediated to a significant degree by the ArsRS two-component system. While *imaA* mRNA was greatly increased at low pH, we did not detect a corresponding increase in ImaA protein levels at low pH. This paradox of increased transcript levels not directly translating to increases in protein levels is not unprecedented in studies of the *H. pylori* ArsRS system. Loh et al. recently examined the proteomes of wild-type *H. pylori* and an isogenic *arsS* mutant under neutral and acidic conditions and compared them to the previously established transcriptional profiles for each strain under these conditions (48). They found very few acid-responsive protein changes in either strain, as only 15 proteins were differentially expressed in total. *imaA* likely belongs to the group of more than 100 genes that show altered transcriptional profiles at low pH but do not exhibit clear changes in protein levels. Loh et al. attributed the discrepancy between transcript and protein levels to posttranscriptional regulatory processes, which may dilute alterations in acid-induced protein expression (48). Despite discrepancies in protein levels, it is clear that ArsS is important for expression of *imaA* at low pH, demonstrating that *imaA* is under the control of the ArsRS regulon.

We show here that ImaA is important for mouse colonization. ImaA was previously found to be crucial for colonization in a different animal model, the gerbil, as part of a global transposon mutagenesis screen done in strain G1.1 that was evaluated in a competition model (37). Thus, these two studies demonstrate that ImaA's presence is necessary to achieve wild-type gastric colonization in multiple animal models. Conversely, a third analyzed strain, SS1, tolerates the loss of *imaA* in murine infections. Of note, strain SS1 does express ImaA (Fig. 3). There are many differences between strain SS1 and strain LSH100/G27, the most notable of which is that SS1 has an inactive *cag*PAI T4SS, while that of G27 and its mouse-selected variants is active (8). Strain G1.1, like SS1, does not secrete CagA (25, 34). Thus, ImaA appears to be important for colonization in both Cag-positive and Cag-negative strains, and furthermore, ImaA may have roles in the host that are not limited to affecting the *cag*PAI, although those remain to be determined.

A rodent colonization defect is unusual with *H. pylori* outer membrane proteins. The *H. pylori* adhesin proteins BabAB or SabA do not display any colonization defects, and AlpAB exhibits a defect that is statistically insignificant (4, 68). In fact, the only characterized *H. pylori* outer membrane protein to display a rodent colonization defect is the autotransporter VacA (64). VacA, like ImaA, possesses immunomodulatory activity albeit through suppression of T-cell activation (13). However, unlike VacA, ImaA appears to act while cell associated, as we were unable to identify an ImaA secreted peptide in cell culture supernatant. Interestingly, it was recently shown that mutants deficient for the laminin binding proteins AlpA and AlpB caused greater levels of inflammation in gerbil infections (68). This outcome, however, was not attributed to any inherent AlpAB immunomodulatory properties but rather the mutant's inability to intimately adhere to gastric epithelial cells and express other immunosuppressive proteins. We were unable to detect any *in vitro* adherence ability associated with ImaA (data not shown), so we believe it operates in a different manner from AlpAB.

A central component of *H. pylori*-induced inflammation is delivery of proinflammatory molecules into host cells via the *cag*PAI T4SS. We have demonstrated that the Δ*imaA*::*cat* mutant evokes a significant increase in expression of the proinflammatory cytokines IL-8, and TNF-α compared to AGS cell infections with wild-type *H. pylori*. While the bulk of the inflammation experiments were done with the *H. pylori* G27 derivative, LSH100, we also found that ImaA had a similar effect in strain 26695, suggesting that ImaA function is conserved. Furthermore, we found that the *imaA* mutant inflammation phenotype requires a functional *cag*PAI T4SS. This outcome suggests that ImaA acts to diminish the normal *cag*PAI-mediated induction of proinflammatory cytokines. The *cag*PAI T4SS aids the delivery of two effectors capable of inducing IL-8 expression in epithelial cells, CagA and peptidoglycan (14, 79). While we do not know how ImaA interacts with the *cag*PAI, it is not unprecedented for *H. pylori* outer membrane

proteins to influence *cag*PAI T4SS activity. The ABO/Lewis b (Le^b) blood group antigen binding protein, BabA, facilitates interactions between the *cag*PAI T4SS machinery and the host cell. Strains null for *babA* induce reduced levels of IL-8 in infected host cells, opposite to what we see in *imaA* mutant infections (33). Interestingly, the protein homology/analogy recognition Engine (PHYRE) predicts that ImaA has homology to the bacterial integrin binding protein, invasin ($E = 1.8 \times 10^{-4}$). Components of the *cag*PAI T4SS pilus bind directly to the $\alpha_5\beta_1$ integrin receptor to facilitate secretion of CagA and peptidoglycan into the host cell cytoplasm (40). Thus, it is possible that ImaA and the *cag*PAI T4SS machinery compete for integrin binding and that in the absence of ImaA, there is increased T4SS binding and therefore, enhanced effector molecule secretion into host cells.

In conclusion, we have determined that the *H. pylori* host-induced *HP0289* gene encodes a surface-localized autotransporter protein that we designate ImaA. ImaA promotes colonization of the host stomach and diminishes the inflammatory response. Specifically, ImaA decreases the amount of *Il8* transcript generated by the *H. pylori cag*PAI. *imaA* expression is furthermore controlled by the acid-sensing two-component regulatory system ArsRS in response to acid. These findings support the notion that genes induced *in vivo* play a central role in *H. pylori* pathogenesis. Furthermore, they suggest that *H. pylori* has sophisticated mechanisms to modulate the host inflammatory response by controlling expression of a protein that decreases bacterially triggered inflammatory gene expression.

ACKNOWLEDGMENTS

We thank David McGee and Kylie Nolan for providing the *H. pylori* SS1 *cagE*::*kan* mutant. We are also grateful to Fitnat Yildiz and Annah Rolig for critical reading of the manuscript.

This work was supported by a Research Scholar Grant (RSG-05-249-01-MBC) from the American Cancer Society (to K.M.O.) and by grant AI050000 (to K.M.O.) from the National Institutes of Allergy and Infectious Disease (NIAID) at the National Institutes of Health.

The contents of this article are solely the responsibility of the authors and do not necessarily represent the official views of the NIH.

REFERENCES

1. **Akopyants NS, Eaton KA, Berg DE.** 1995. Adaptive mutation and co-colonization during Helicobacter pylori infection of gnotobiotic piglets. Infect. Immun. **63**:116–121.
2. **Algood HM, Gallo-Romero J, Wilson KT, Peek RM, Cover TL.** 2007. Host response to Helicobacter pylori infection before initiation of the adaptive immune response. FEMS Immunol. Med. Microbiol. **51**:577–586.
3. **Alm RA, et al.** 2000. Comparative genomics of Helicobacter pylori: analysis of the outer membrane protein families. Infect. Immun. **68**:4155–4168.
4. **Amieva MR, El-Omar EM.** 2008. Host-bacterial interactions in Helicobacter pylori infection. Gastroenterology **134**:306–323.
5. **Ashgar SS, et al.** 2007. CapA, an autotransporter protein of Campylobacter jejuni, mediates association with human epithelial cells and colonization of the chicken gut. J. Bacteriol. **189**:1856–1865.
6. **Bach S, Makristathis A, Rotter M, Hirschl AM.** 2002. Gene expression profiling in AGS cells stimulated with Helicobacter pylori isogenic strains (cagA positive or cagA negative). Infect. Immun. **70**:988–992.
7. **Baik SC, et al.** 2004. Proteomic analysis of the sarcosine-insoluble outer membrane fraction of Helicobacter pylori strain 26695. J. Bacteriol. **186**:949–955.
8. **Baldwin DN, et al.** 2007. Identification of Helicobacter pylori genes that contribute to stomach colonization. Infect. Immun. **75**:1005–1016.
9. **Beier D, Frank R.** 2000. Molecular characterization of two-component systems of Helicobacter pylori. J. Bacteriol. **182**:2068–2076.
10. **Bendtsen JD, Nielsen H, von Heijne G, Brunak S.** 2004. Improved prediction of signal peptides: SignalP 3.0. J. Mol. Biol. **340**:783–795.
11. **Benz I, Schmidt MA.** 2011. Structures and functions of autotransporter proteins in microbial pathogens. Int. J. Med. Microbiol. **301**:461–468.
12. **Blaser MJ.** 1997. The versatility of Helicobacter pylori in the adaptation to the human stomach. J. Physiol. Pharmacol. **48**:307–314.
13. **Boncristiano M, et al.** 2003. The Helicobacter pylori vacuolating toxin inhibits T cell activation by two independent mechanisms. J. Exp. Med. **198**:1887–1897.
14. **Brandt S, Kwok T, Hartig R, König W, Backert S.** 2005. NF-kappaB activation and potentiation of proinflammatory responses by the Helicobacter pylori CagA protein. Proc. Natl. Acad. Sci. U. S. A. **102**:9300–9305.
15. **Bron PA, Grangette C, Mercenier A, de Vos WM, Kleerebezem M.** 2004. Identification of Lactobacillus plantarum genes that are induced in the gastrointestinal tract of mice. J. Bacteriol. **186**:5721–5729.
16. **Camilli A, Mekalanos JJ.** 1995. Use of recombinase gene fusions to identify Vibrio cholerae genes induced during infection. Mol. Microbiol. **18**:671–683.
17. **Castillo AR, Woodruff AJ, Connolly LE, Sause WE, Ottemann KM.** 2008. Recombination-based in vivo expression technology identifies Helicobacter pylori genes important for host colonization. Infect. Immun. **76**:5632–5644.
18. **Chevalier C, Thiberge JM, Ferrero RL, Labigne A.** 1999. Essential role of Helicobacter pylori gamma-glutamyltranspeptidase for the colonization of the gastric mucosa of mice. Mol. Microbiol. **31**:1359–1372.
19. **Covacci A, et al.** 1993. Molecular characterization of the 128-kDa immunodominant antigen of Helicobacter pylori associated with cytotoxicity and duodenal ulcer. Proc. Natl. Acad. Sci. U. S. A. **90**:5791–5795.
20. **Dautin N, Barnard T, Anderson D, Bernstein H.** 2007. Cleavage of a bacterial autotransporter by an evolutionarily convergent autocatalytic mechanism. EMBO J. **26**:1942–1952.
21. **Day AS, et al.** 2000. cagE is a virulence factor associated with Helicobacter pylori-induced duodenal ulceration in children. J. Infect. Dis. **181**:1370–1375.
22. **Donahue JP, Israel DA, Peek RM, Blaser MJ, Miller GG.** 2000. Overcoming the restriction barrier to plasmid transformation of Helicobacter pylori. Mol. Microbiol. **37**:1066–1074.
23. **Dossumbekova A, et al.** 2006. Helicobacter pylori outer membrane proteins and gastric inflammation. Gut **55**:1360–1361.
24. **Eaton KA, Benson LH, Haeger J, Gray BM.** 2006. Role of transcription factor T-bet expression by CD4+ cells in gastritis due to Helicobacter pylori in mice. Infect. Immun. **74**:4673–4684.
25. **Eaton KA, et al.** 2001. Role of Helicobacter pylori cag region genes in colonization and gastritis in two animal models. Infect. Immun. **69**:2902–2908.
26. **Finn RD, et al.** 2010. The Pfam protein families database. Nucleic Acids Res. **38**:D211–D222.
27. **Harris AG, et al.** 2003. Catalase (KatA) and KatA-associated protein (KapA) are essential to persistent colonization in the Helicobacter pylori SS1 mouse model. Microbiology **149**:665–672.
28. **Henderson I, Nataro J.** 2001. Virulence functions of autotransporter proteins. Infect. Immun. **69**:1231–1243.
29. **Henderson I, Navarro-Garcia F, Desvaux M, Fernandez R, Ala'Aldeen D.** 2004. Type V protein secretion pathway: the autotransporter story. Microbiol. Mol. Biol. Rev. **68**:692–744.
30. **Herrera V, Parsonnet J.** 2009. Helicobacter pylori and gastric adenocarcinoma. Clin. Microbiol. Infect. **15**:971–976.
31. **Huang J, O'Toole PW, Doig P, Trust TJ.** 1995. Stimulation of interleukin-8 production in epithelial cell lines by Helicobacter pylori. Infect. Immun. **63**:1732–1738.
32. **Ilver D, et al.** 1998. Helicobacter pylori adhesin binding fucosylated histo-blood group antigens revealed by retagging. Science **279**:373–377.
33. **Ishijima N, et al.** 2011. BabA-mediated adherence is a potentiator of the Helicobacter pylori type IV secretion system activity. J. Biol. Chem. **286**:25256–25264.
34. **Israel DA, et al.** 2001. Helicobacter pylori strain-specific differences in genetic content, identified by microarray, influence host inflammatory responses. J. Clin. Invest. **107**:611–620.
35. **Janakiraman A, Slauch JM.** 2000. The putative iron transport system SitABCD encoded on SPI1 is required for full virulence of Salmonella typhimurium. Mol. Microbiol. **35**:1146–1155.
36. **Janzon A, et al.** 2009. Presence of high numbers of transcriptionally active

Helicobacter pylori in vomitus from Bangladeshi patients suffering from acute gastroenteritis. Helicobacter **14**:237–247.
37. **Kavermann H, et al.** 2003. Identification and characterization of Helicobacter pylori genes essential for gastric colonization. J. Exp. Med. **197**:813–822.
38. **Kawai M, et al.** 2011. Evolution in an oncogenic bacterial species with extreme genome plasticity: Helicobacter pylori East Asian genomes. BMC Microbiol. **11**:104. doi:10.1186/1471-2180-11-104.
39. **Kuipers EJ, et al.** 1995. Long-term sequelae of Helicobacter pylori gastritis. Lancet **345**:1525–1528.
40. **Kwok T, et al.** 2007. Helicobacter exploits integrin for type IV secretion and kinase activation. Nature **449**:862–866.
41. **Lamb A, et al.** 2009. Helicobacter pylori CagA activates NF-kappaB by targeting TAK1 for TRAF6-mediated Lys 63 ubiquitination. EMBO Rep. **10**:1242–1249.
42. **Lee A, et al.** 1997. A standardized mouse model of Helicobacter pylori infection: introducing the Sydney strain. Gastroenterology **112**:1386–1397.
43. **Lee KH, et al.** 2004. Alanine-threonine polymorphism of Helicobacter pylori RpoB is correlated with differential induction of interleukin-8 in MKN45 cells. J. Clin. Microbiol. **42**:3518–3524.
44. **Lee SH, Butler SM, Camilli A.** 2001. Selection for in vivo regulators of bacterial virulence. Proc. Natl. Acad. Sci. U. S. A. **98**:6889–6894.
45. **Lenz JD, et al.** 2011. Expression during host infection and localization of Yersinia pestis autotransporter proteins. J. Bacteriol. **193**:5936–5949.
46. **Lin LF, Posfai J, Roberts RJ, Kong H.** 2001. Comparative genomics of the restriction-modification systems in Helicobacter pylori. Proc. Natl. Acad. Sci. U. S. A. **98**:2740–2745.
47. **Livak KJ, Schmittgen TD.** 2001. Analysis of relative gene expression data using real-time quantitative PCR and the 2(−Delta Delta C(T)) method. Methods **25**:402–408.
48. **Loh JT, Gupta SS, Friedman DB, Krezel AM, Cover TL.** 2010. Analysis of protein expression regulated by the Helicobacter pylori ArsRS two-component signal transduction system. J. Bacteriol. **192**:2034–2043.
49. **Lowe AM, Beattie DT, Deresiewicz RL.** 1998. Identification of novel staphylococcal virulence genes by in vivo expression technology. Mol. Microbiol. **27**:967–976.
50. **Lowenthal AC, et al.** 2009. Functional analysis of the Helicobacter pylori flagellar switch proteins. J. Bacteriol. **191**:7147–7156.
51. **Mahdavi J, et al.** 2002. Helicobacter pylori SabA adhesin in persistent infection and chronic inflammation. Science **297**:573–578.
52. **Marchetti M, Rappuoli R.** 2002. Isogenic mutants of the cag pathogenicity island of Helicobacter pylori in the mouse model of infection: effects on colonization efficiency. Microbiology **148**:1447–1456.
53. **Merrell DS, Goodrich ML, Otto G, Tompkins LS, Falkow S.** 2003. pH-regulated gene expression of the gastric pathogen Helicobacter pylori. Infect. Immun. **71**:3529–3539.
54. **Montecucco C, Rappuoli R.** 2001. Living dangerously: how Helicobacter pylori survives in the human stomach. Nat. Rev. Mol. Cell Biol. **2**:457–466.
55. **Nazarenko I, et al.** 2002. Multiplex quantitative PCR using self-quenched primers labeled with a single fluorophore. Nucleic Acids Res. **30**:e37. doi:10.1093/nar/30.9.e37.
56. **Obonyo M, Guiney DG, Harwood J, Fierer J, Cole SP.** 2002. Role of gamma interferon in Helicobacter pylori induction of inflammatory mediators during murine infection. Infect. Immun. **70**:3295–3299.
57. **Ottemann KM, Lowenthal AC.** 2002. Helicobacter pylori uses motility for initial colonization and to attain robust infection. Infect. Immun. **70**:1984–1990.
58. **Pappo J, et al.** 1999. Helicobacter pylori infection in immunized mice lacking major histocompatibility complex class I and class II functions. Infect. Immun. **67**:337–341.
59. **Pflock M, Dietz P, Schär J, Beier D.** 2004. Genetic evidence for histidine kinase HP165 being an acid sensor of Helicobacter pylori. FEMS Microbiol. Lett. **234**:51–61.
60. **Pflock M, et al.** 2006. Characterization of the ArsRS regulon of Helicobacter pylori, involved in acid adaptation. J. Bacteriol. **188**:3449–3462.
61. **Pflock M, Kennard S, Delany I, Scarlato V, Beier D.** 2005. Acid-induced activation of the urease promoters is mediated directly by the ArsRS two-component system of Helicobacter pylori. Infect. Immun. **73**:6437–6445.
62. **Pflock M, Kennard S, Finsterer N, Beier D.** 2006. Acid-responsive gene regulation in the human pathogen Helicobacter pylori. J. Biotechnol. **126**:52–60.
63. **Sabarth N, et al.** 2005. Identification of Helicobacter pylori surface proteins by selective proteinase K digestion and antibody phage display. J. Microbiol. Methods **62**:345–349.
64. **Salama NR, Otto G, Tompkins L, Falkow S.** 2001. Vacuolating cytotoxin of Helicobacter pylori plays a role during colonization in a mouse model of infection. Infect. Immun. **69**:730–736.
65. **Sauri A, et al.** 2009. The Bam (Omp85) complex is involved in secretion of the autotransporter haemoglobin protease. Microbiology **155**:3982–3991.
66. **Saviola B, Woolwine SC, Bishai WR.** 2003. Isolation of acid-inducible genes of Mycobacterium tuberculosis with the use of recombinase-based in vivo expression technology. Infect. Immun. **71**:1379–1388.
67. **Schultz J, Milpetz F, Bork P, Ponting CP.** 1998. SMART, a simple modular architecture research tool: identification of signaling domains. Proc. Natl. Acad. Sci. U. S. A. **95**:5857–5864.
68. **Senkovich OA, et al.** 2011. Helicobacter pylori AlpA and AlpB bind host laminin and influence gastric inflammation in gerbils. Infect. Immun. **79**:3106–3116.
69. **Sharma CM, et al.** 2010. The primary transcriptome of the major human pathogen Helicobacter pylori. Nature **464**:250–255.
70. **Shibata J, et al.** 1999. Regulation of tumour necrosis factor (TNF) induced apoptosis by soluble TNF receptors in Helicobacter pylori infection. Gut **45**:24–31.
71. **Slauch JM, Camilli A.** 2000. IVET and RIVET: use of gene fusions to identify bacterial virulence factors specifically induced in host tissues. Methods Enzymol. **326**:73–96.
72. **Styer CM, et al.** 2010. Expression of the BabA adhesin during experimental infection with Helicobacter pylori. Infect. Immun. **78**:1593–1600.
73. **Suerbaum S, Michetti P.** 2002. Helicobacter pylori infection. N. Engl. J. Med. **347**:1175–1186.
74. **Terry K, Williams SM, Connolly L, Ottemann KM.** 2005. Chemotaxis plays multiple roles during Helicobacter pylori animal infection. Infect. Immun. **73**:803–811.
75. **Testerman TL, McGee DJ, Mobley HL.** 2001. Helicobacter pylori growth and urease detection in the chemically defined medium Ham's F-12 nutrient mixture. J. Clin. Microbiol. **39**:3842–3850.
76. **Tomb JF, et al.** 1997. The complete genome sequence of the gastric pathogen Helicobacter pylori. Nature **388**:539–547.
77. **Van Gerven N, Sleutel M, Deboeck F, De Greve H, Hernalsteens JP.** 2009. Surface display of the receptor-binding domain of the F17a-G fimbrial adhesin through the autotransporter AIDA-I leads to permeability of bacterial cells. Microbiology **155**:468–476.
78. **Veal-Carr WL, Stibitz S.** 2005. Demonstration of differential virulence gene promoter activation in vivo in Bordetella pertussis using RIVET. Mol. Microbiol. **55**:788–798.
79. **Viala J, et al.** 2004. Nod1 responds to peptidoglycan delivered by the Helicobacter pylori cag pathogenicity island. Nat. Immunol. **5**:1166–1174.
80. **Watanabe T, et al.** 2010. NOD1 contributes to mouse host defense against Helicobacter pylori via induction of type I IFN and activation of the ISGF3 signaling pathway. J. Clin. Invest. **120**:1645–1662.
81. **Wen Y, Feng J, Scott DR, Marcus EA, Sachs G.** 2007. The HP0165-HP0166 two-component system (ArsRS) regulates acid-induced expression of HP1186 alpha-carbonic anhydrase in Helicobacter pylori by activating the pH-dependent promoter. J. Bacteriol. **189**:2426–2434.
82. **Williams CL, Haines R, Cotter PA.** 2008. Serendipitous discovery of an immunoglobulin-binding autotransporter in Bordetella species. Infect. Immun. **76**:2966–2977.
83. **Williams SM, et al.** 2007. Helicobacter pylori chemotaxis modulates inflammation and bacterium-gastric epithelium interactions in infected mice. Infect. Immun. **75**:3747–3757.
84. **Yamaoka Y, et al.** 2002. Helicobacter pylori infection in mice: role of outer membrane proteins in colonization and inflammation. Gastroenterology **123**:1992–2004.
85. **Yamaoka Y, et al.** 1997. Induction of various cytokines and development of severe mucosal inflammation by cagA gene positive Helicobacter pylori strains. Gut **41**:442–451.
86. **Yamaoka Y, Kwon DH, Graham DY.** 2000. A M(r) 34,000 proinflammatory outer membrane protein (oipA) of Helicobacter pylori. Proc. Natl. Acad. Sci. U. S. A. **97**:7533–7538.